ELSEVIER

Ceramics International 30 (2004) 1961–1965

CERAMICS INTERNATIONAL

www.elsevier.com/locate/ceramint

Effect of fluorine addition on the corrosion resistance of hydroxyapatite ceramics

Yanming Chen, Xigeng Miao*

School of Materials Engineering, Nanyang Technological University, Nanyang Avenue, Nanyang 639798, Singapore

Received 12 November 2003; received in revised form 12 December 2003; accepted 23 December 2003

Available online 8 May 2004

Abstract

Synthetic hydroxyapatite (HA) ceramics have found their important biomedical applications as bone implants and bone substitutes. However, the bioactivity and the biostability of HA still need to be tailored for specific applications. To improve the biostability of HA, fluorine addition to HA ceramics to form fluorine-substituted hydroxyapatite (FHA) is a solution. While the preparation and processing of FHA powders have been found in the literature, this study aimed to investigate the effect of fluorine content on the corrosion resistance (an indication of biostability) of the FHA ceramics. The FHA powders with compositions of $Ca_{10}(PO_4)_6(OH)_{2(1-x)}F_{2x}$ ($x = 0$, 0.2, 0.4, 0.8) were prepared by a wet precipitation method. By sintering the particle compacts at 1200 °C in air, all the FHA ceramics reached more than 95% of their theoretical densities. The FHA ceramics with different fluorine contents were then immersed in a 5 wt.% citric acid solution for 10 min. Transmission electron microscopy (TEM) results showed that the FHA powders produced were needle-like nanoparticles with a width of 80 nm and a length of 20 nm. Scanning electron microscopy (SEM) results indicated that increasing fluorine content led to increasing corrosion resistance of the FHA ceramics. The increased corrosion resistance of the FHA ceramics compared with the pure HA ceramics suggested the biostability of the FHA ceramics in vitro and in vivo and thus the long-term performance of implants made of the FHA compositions.

Keywords: Hydroxyapatite; Fluoroapatite

1. Introduction

Hydroxyapatite (HA, $Ca_{10}(PO_4)_6(OH)_2$) has been extensively investigated as a bone implant material due to its excellent biocompatibility [1]. HA is also one of the few materials that form strong chemical bond with bone in vivo. However, its poor thermostability (i.e., decomposition at high temperatures) and subsequent high dissolution rate in a biological environment has, to some extent, limited its applications. On the other hand, fluorine is known to be very important in influencing the physical and biological properties of HA and in the treatment of osteoporosis [2]. Unlike HA, which normally decomposes to tricalcium phosphate (TCP, $Ca_3(PO_4)_2$) at above 1200 °C, fluorine-substituted HA (FHA, $Ca_{10}(PO_4)_6(OH)_2-_{2x}F_{2x}$) has shown phase stability even up to higher temperatures. The improved thermal stability is mainly because that the substitution of F^- for OH^- causes a contraction in the *a*-axis dimension without changing the *c*-axis dimension, resulting in an increase in the crystallinity and in the stability. However, pure fluoroapatite (FA, $Ca_{10}(PO_4)_6F_2$) rather than fluorine-substituted HA, could not be a good biomaterial because it was too stable and seemed not to give osteoconduction [3]. Moreover, pure FA might be toxic since the fluorine content in FA (3.77 wt.%) is much higher than that in human bone (<1.00 wt.%).

Recently, FHA has received great interest and its preparation methods have been widely studied [4–8]. Wet chemical precipitation and sol–gel method are generally used to prepare fine FHA powders because the former is technically simple and commercially efficient while the latter is capable of producing more homogeneous powders. Various preparation parameters have been investigated for the FHA synthesis. Moztarzadeh and Salahi [9] stated that different pH value ranges of the staring solutions resulted in different phases after the precipitation. Jha et al. [6] proposed that increasing fluoride ion concentration tended to reduce the

* Corresponding author. Fax: +65-6790-9081.
E-mail address: asxgmiao@ntu.edu.sg (X. Miao).

0272-8842/$30.00
doi:10.1016/j.ceramint.2003.12.182

aspect ratio of the crystallites. Okazaki et al. [5,8,10] have studied different types of heterogeneous FHA synthesized by varying the fluoride supply step during the experimental period and reported that the fluoride supply step greatly affected the solubility behavior of FHA.

However, most literature so far has focused on the preparation and processing of FHA powders. The preparation of FHA ceramics and the effect of fluorine content on the corrosion resistance of FHA ceramics have not been systematically studied. Thus, in the present study, nano-sized FHA powders with different fluorine contents were prepared by a wet chemical precipitation method. The powders were then pressed and sintered in air at 1200 °C. The effect of the fluorine content on the corrosion resistance of FHA ceramics was subsequently investigated.

2. Experimental procedure

2.1. Sample preparation

Calcium nitrate 4-hydrate ($Ca(NO_3)_2{\cdot}4H_2O$, AnalarR grade, BDH Limited Company, Inc.), diammonium hydrogen phosphate ($(NH_4)_2HPO_4$, Merck KgaA Company, Inc.), and ammonium fluoride (NH_4F, Fluka Chemie Company, Inc.) were used as the starting chemicals for calcium, phosphorus, and fluorine precursors. For the preparation of FHA fine powder, calcium nitrate 4-hydrate was first dissolved in distilled water and was vigorously stirred on a hotplate to form a 0.5 M solution. Diammonium hydrogen phosphate aqueous solution was then added dropwise into the calcium nitrate 4-hydrate solution to achieve a Ca/P ratio of 1.67. Then, ammonium fluoride solution was added in to the constantly stirred solution containing Ca and P ions. Different amounts of the ammonium fluoride solution were added individually to control the amount of x in the formula of $Ca_{10}(PO_4)_6(OH)_{2-2x}F_{2x}$. When the x in the $Ca_{10}(PO_4)_6(OH)_{2-2x}F_{2x}$ formula was 0, 0.2, 0.4, and 0.6, respectively, the subsequently obtained powders were named HA, HA02F, HA04F, and HA06F, respectively. The mixed solution was clear so far; no precipitation occurred. To obtain the FHA precipitates, an ammonia solution was dropped into the mixed solution to adjust the pH value of the mixed solution to 10–11. This was followed by constant stirring for 2 h. The solution with the precipitates was then kept still for 24 h before the supernatant solution was discarded and the precipitates were washed several times with distilled water to remove residual ions. The washed precipitates (powder) were dried in air and crushed by ball milling with ethanol for 1 h, followed by drying again in oven. The dried pieces of powder cakes were ground into fine powders using a vibrating dry mill. The as-prepared powders were then axially pressed at 300 MPa in a 13-mm steel die. The pressed pellets were sintered in air at 1200 °C for 1 h with a heating rate of 5 °C/min and a cooling rate of 10 °C/min.

2.2. Sample characterization

The FHA powders and the sintered FHA ceramic bodies were characterized using X-ray diffraction (XRD, Lab XRD-6000 Shimadzu), scanning electron microscopy (SEM, JEOL, JSM-5410 LV), transmission electron microscopy (TEM, JEM-2010), and Vickers microhardness tester (Matsuzawa MXT70). XRD data of FHA powders and sintered bodies were collected from 20° to 60° (2θ angle) using the monochromatic Cu Kα radiation at the step of 0.02° with a counting time of 1 s per step. The morphology of the FHA powders was observed by TEM. For TEM observation, carbon-coated 200 mesh copper grids were dipped in a dilute FHA suspension. The excess suspension on the copper grids was carefully removed using an absorbent paper, followed by drying in air. The FHA powders on the copper grids were then examined using TEM in the bright field mode with an accelerating voltage of 100 kV.

The densities of the sintered FHA bodies were calculated using the formula of density = weight/volume. For every sample type, the dimensions and weights of five samples were taken. The density of individual sample was then calculated, and the average was taken. To evaluate the chemical stability of the FHA ceramics, the FHA ceramic samples were polished and then immersed in a 5 wt.% citric acid solution for 10 min prior to observation of surface morphology using SEM. Finally, the Vickers microhardness was measured on finely polished surfaces of FHA sintered bodies with an indentation load of 500 g and a holding time of 25 s. After indentation, the diagonal lengths of the diamond-shaped impressions were measured using the microscope attached to the hardness tester. The hardness values were automatically given by the instrument by using the formula of $H_v = 1.8544P/(2a)^2$, where H_v is the Vickers microhardness value, P the indentation load (kg), and $2a$ the average diagonal length of the indentation impression (mm).

3. Results and discussion

The XRD patterns of the FHA powders are shown in Fig. 1 with the distinct peaks at 26°, 32°, 40°, and 50°, being characteristic of apatite phase. The slight shift of (2 1 1) and (1 1 2) peaks to the right hand side indicates the substitution of OH^- with F^- in the HA matrix, as such substitution tended to decrease the α-axis length of the HA lattice. Fig. 2 shows the transmission electron micrographs of HA and FHA powders. The HA and FHA particles are elongated with about 80 nm in length and 20 nm in width. The substitution of F^- for OH^- in the host HA crystals does not significantly affect the morphology of the HA particles.

All the FHA ceramics sintered at 1200 °C have reached densities over 95% theoretical density; they are 96.2, 95.7, 95.0, and 95.5%, respectively. Fig. 3 is the XRD patterns of HA, HA02, HA04, and HA06F samples sintered at 1200 °C for 1 h, respectively. The peaks observed are similar to those

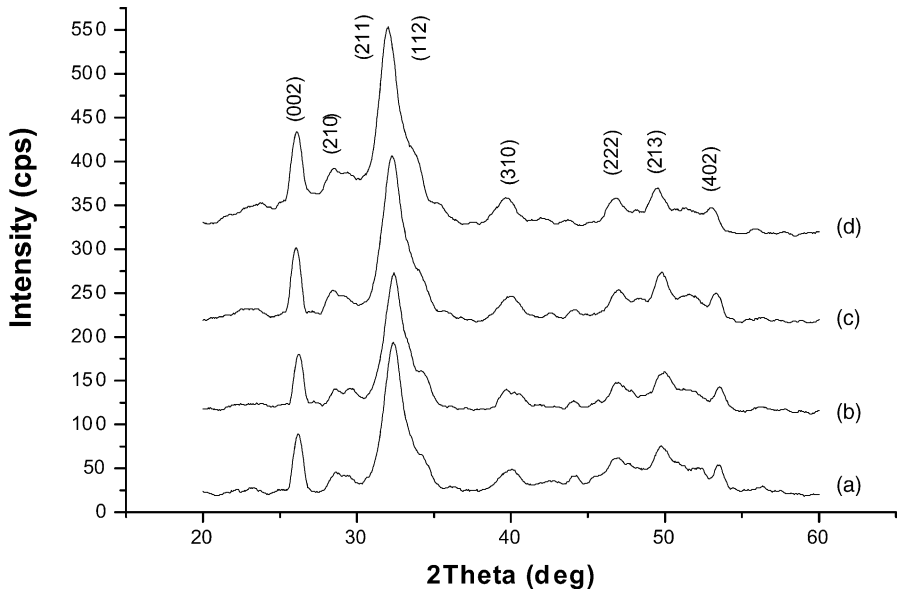

Fig. 1. XRD patterns of (a) HA, (b) HA02F, (c) HA04F, and (d) HA06F powders.

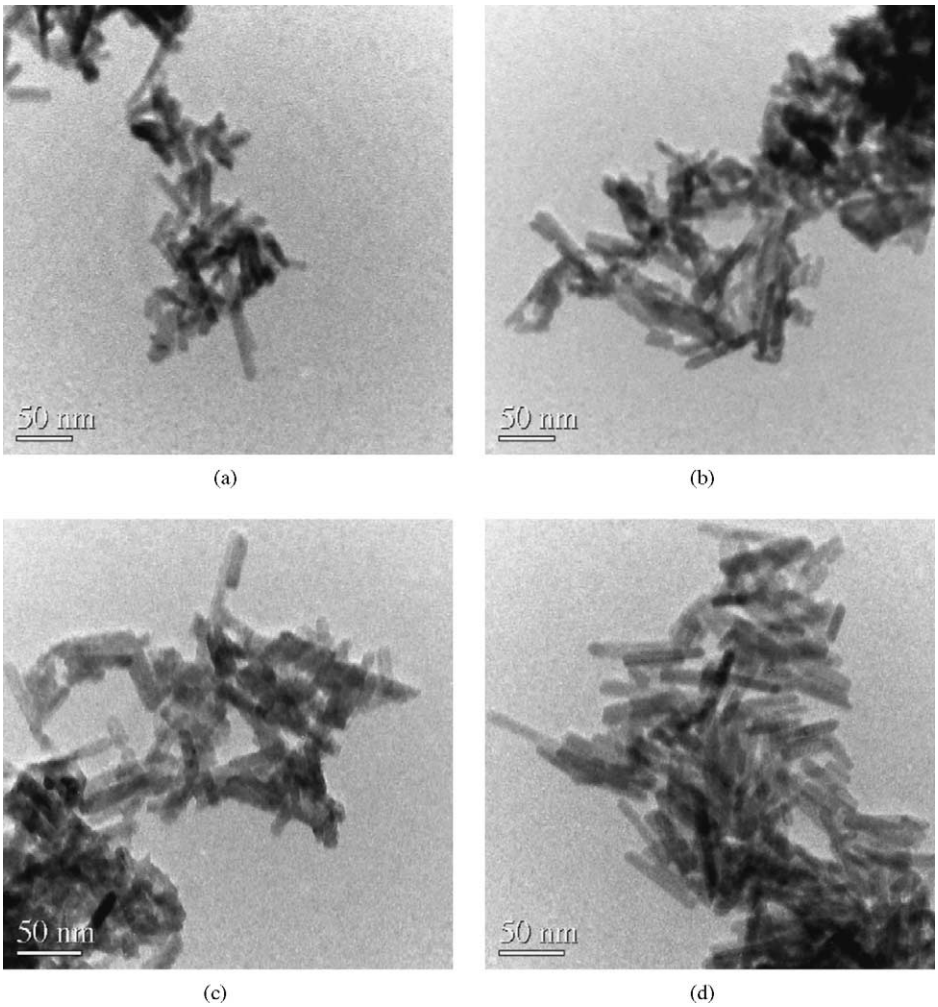

Fig. 2. TEM micrographs showing the particle morphologies of (a) HA, (b) HA02F, (c) HA04F, and (d) HA06F powders.

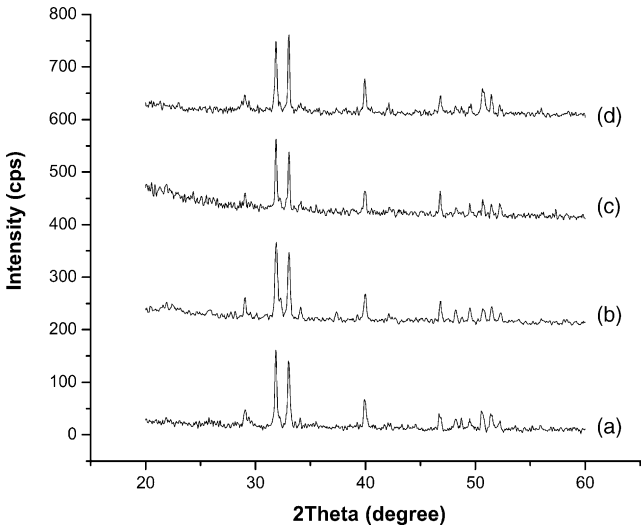

Fig. 3. XRD patterns of (a) HA, (b) HA02F, (c) HA04F, and (d) HA06F sintered at 1200 °C.

of the starting FHA powders (Fig. 1), except for the shape of the peaks of the sintered ceramics, which is mainly due to the increased crystallinity of the FHA apatite grains or crystals. No other phases, such as alpha-tricalcium phosphate (α-TCP), beta-tricalcium phosphate (β-TCP), and/or tetra-calcium phosphate (TTCP), are identified in Fig. 3.

The different FHA samples sintered at 1200 °C were polished and chemically etched by the 5 wt.% citric acid solution to evaluate the chemical stability of the sintered FHA ceramics. The surface morphologies of the samples after etching are presented in Fig. 4.

By comparing Fig. 4a–d, one can find that with the increasing fluorine content, the surface of the FHA ceramics is smoother and less corroded by the citric acid solution. This observation indicates higher corrosion resistance in FHA ceramics when the fluorine content is higher. The positive effect of fluoride on the corrosion resistance of the FHA ceramics can be explained by considering the crystal structure. In HA, the hydrogen atoms are arranged in atomic interstices neighboring to the oxygen atoms and are oriented randomly, which confers a certain disorder to the crystal structure of

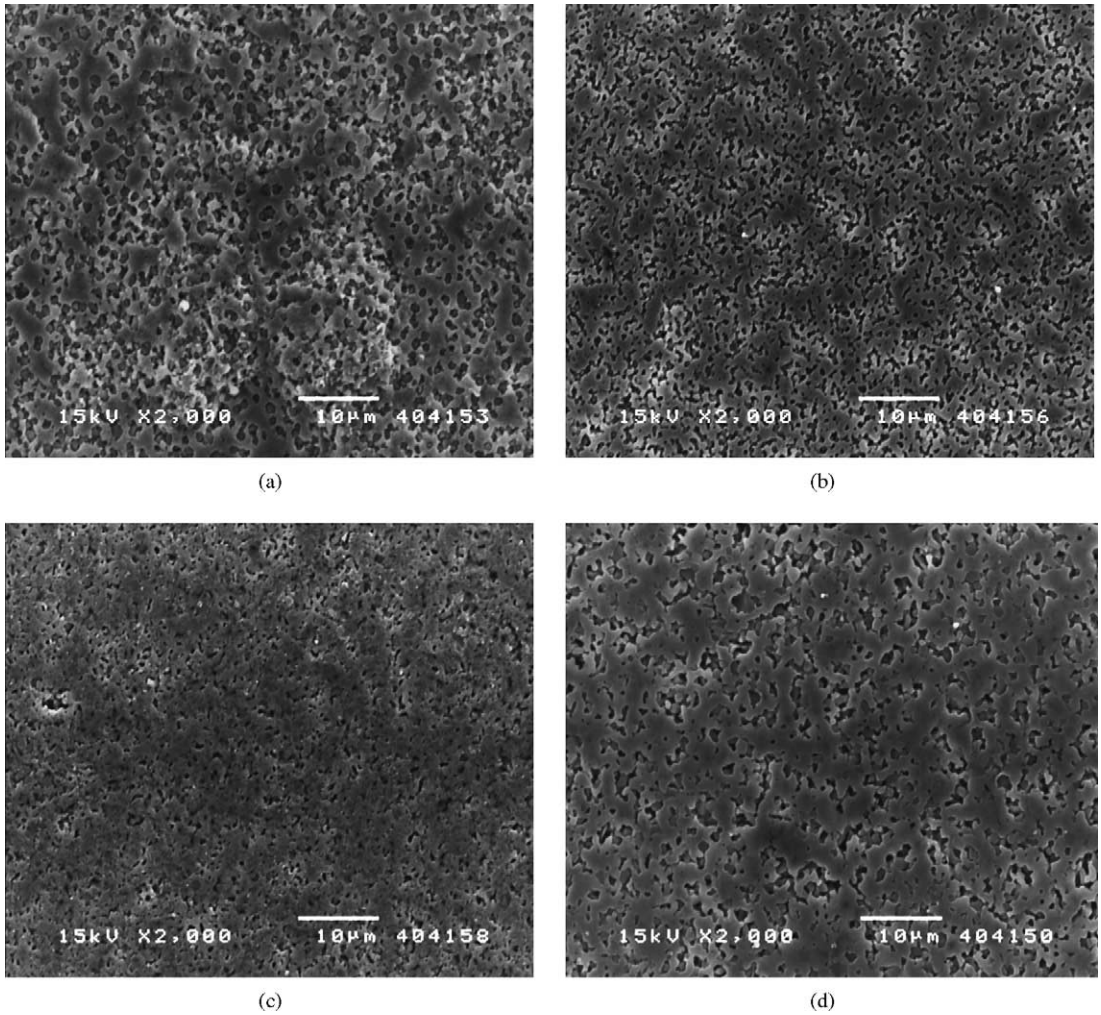

Fig. 4. SEM micrographs of the polished and etched surfaces of (a) HA, (b) HA02F, (c) HA04F, and (d) HA06F sintered samples.

HA. Once the OH^- ions are partially substituted by the F^- ones, the existing hydrogen atoms of the OH^- group are tightly bound to the nearby F^- anions because of the higher affinity of the fluoride in respect to the oxygen, producing a quite well-ordered apatite structure, which causes the increases of the chemical stability of the HA matrix.

The Vickers microhardness values of the HA, HA02F, HA04F, and HA06F samples sintered at 1200 °C are 5.81 ± 0.35 GPa, 6.03 ± 0.31 GPa, 5.97 ± 0.27 GPa, and 6.10 ± 0.39 GPa, respectively. Thus, the substitution of the OH^- ions with the F^- ions in the host HA has slightly increased the Vickers microhardness of the HA matrix. Thus, fluoride addition has the effect to increase the chemical stability and mechanical property of HA. The future work is to do cell culture in vitro assessment to determine the highest allowable fluorine content without loss of biocompatibility.

4. Conclusions

Both HA ($Ca_{10}(PO_4)_6(OH)_2$) and fluorine-substituted hydroxyapatite (FHA; $Ca_{10}(PO_4)_6(OH)_{2-2x}F_{2x}$, where $0 < x < 1$) crystalline powders with nanometers in particle size and with elongated shapes were prepared by using calcium nitrate 4-hydrate ($Ca(NO_3)_2{\cdot}4H_2O$), diammonium hydrogen phosphate ($(NH_4)_2HPO_4$), and ammonium fluoride (NH_4F) dissolved in water and adjusted to pH 10–11. The green compacts of the fine HA and FHA powders were able to reach greater than 95% theoretical densities after sintering at 1200 °C for only 1 h. The substitution of hydroxyl (OH^-) ions with fluorine (F^-) ions in the HA resulted in FHA ($Ca_{10}(PO_4)_6(OH)_{2-2x}F_{2x}$, where $0 < x < 1$), which showed increased crystallinity, higher corrosion resistance, slightly improved hardness, compared with pure HA.

Acknowledgements

The authors would like to thank the Nanyang Technological University for the provision of the financial support (AcRF RG26/01).

References

[1] M. Jarcho, C.H. Bolen, M.B. Thomas, J. Bobick, J.F. Kay, R.M. Doremus, Hydroxyapatite synthesis and characterization in dense polycrystalline form, J. Mater. Sci. 11 (1976) 2027–2035.
[2] M. Sivakumar, I. Manjubala, Preparation of hydroxyapatite/fluoroapatite–zirconia composites using Indian corals for biomedical applications, Mater. Lett. 50 (2001) 199–205.
[3] E. Adolfsson, M. Nygren, L. Hermansson, Decomposition mechanisms in aluminum oxide–apatite systems, J. Am. Ceram. Soc. 82 (1999) 2909–2912.
[4] K. Cheng, G. Shen, W. Weng, G. Han, J.M.F. Ferreira, J. Yang, Synthesis of hydroxyapatite/fluoroapatite solid solution by a sol–gel method, Mater. Lett. 51 (2001) 37–41.
[5] M. Okazaki, H. Tohda, T. Yanagisawa, M. Taira, J. Takahashi, Differences in solubility of two types of heterogeneous fluoridated hydroxyapatite, Biomaterials 19 (1998) 611–616.
[6] L.J. Jha, S.M. Best, J.C. Knowles, I. Rehman, J.D. Santo, W. Bonfield, Preparation and characterization of fluoride-substituted apatites, J. Mater. Sci.: Mater. Med. 8 (1997) 185–191.
[7] M. Manjubala, S. Sivakumar, N. Nikkath, Synthesis and characterization of hydroxyl/fluoroapatite solid solution, J. Mater. Sci. 36 (2001) 5481–5486.
[8] M. Okazaki, Y. Miake, H. Tohda, T. Yanagisawa, J. Takahashi, Fluoridated apatite synthesized using a multi-step fluoride supply system, Biomaterials 20 (1999) 1303–1307.
[9] F. Moztarzadeh, E. Salahi, Study of conditions of synthesis of calcium phosphate bioceramics, J. Sci. Tech. 10 (1998) 7–14.
[10] M. Okazaki, Y. Miake, H. Tohda, T. Yanagisawa, T. Matsumoto, J. Takahashi, Functionally graded fluoridated apatites, Biomaterials 20 (1999) 1421–1426.